MECHANICALLY INDUCED PHASE TRANSFORMATION IN Al-Cu- Fe-Cr DECAGONAL QUASICRYSTALLINE ALLOY BY HIGH-ENERGY BALL MILLING

T.P. Yadav [1ξ], N.K. Mukhopadhyay[2], R.S. Tiwari[1], O.N. Srivastava[1]

[1]Department of Physics, Banaras Hindu University, Varanasi-221 005, India

[2]Department of Metallurgical Engineering, Institute of Technology, Banaras Hindu University, Varanasi-221 005, India

Keywords: Quasicrystal, Ball milling, Phase transformation, Decagonal phase, B2 phase

Abstract

In the present investigation, an Al-Cu-Fe-Cr decagonal quasicrystalline alloy synthesized by a slow cooling technique, has been mechanically milled in a high-energy ball mill for various times ranging up to 100 h under liquid hexane medium at the speed of 400 rpm with a ball to powder ratio of 40:1. After milling, the milled product has been characterized in order to understand the evolution of the various metastable phases by using X-ray diffraction, scanning electron microscopy and transmission electron microscopy. Powders milled for more than 10 h contained predominantly the B2-type crystalline phase with a lattice parameter of ~ 0.29 nm. No amorphous phase could be identified after a prolonged milling up to 100 h. The disordering in the transformed crystalline phased could be observed. The mechanical stability during milling and the evolution nano phases will be discussed with reference to their relative stability.

Introduction

Non-equilibrium processing techniques can be used successfully to design materials with structures desirable for technological applications [1-3]. Among these, mechanical milling (MM) process has attracted the attention because of its potential as an effective processing route in nanoscience and technology. This technique has been reported for synthesizing the bulk nanocrystalline and amorphous materials from alloys from immiscible systems and intermetallic compounds [4-5]. The energy of the milling is a very important factor for the synthesis of nano crystalline materials and obviously it depends on the milling media, internal mechanics of the specific mill, the power supplied to drive the milling process, and the composition, size, and size distribution of the balls [6].

Ternary Al based alloys have been extensively studied recently for developing as high temperature materials for industrial application [7]. In addition to the complex crystalline phases such as Laves phase, topologically closed packed phase, vacancy ordered phases, the quasicrystalline phases also appear in many systems. It is found that many of the complex crystalline phases are related to quasicrystalline phases. Quasicrystalline material, which was originally discovered in Al-Mn alloy [8], is now considered as a new class of intermetallic compound exhibiting a long range quasiperiodic translational and orientational order [9-10]. After the first report of the metastable quasicrystal (QC) in Al-Mn alloy, Tsai et al [11] discovered the stable icosahedral quasicrystal in Al-Cu-Fe system. Since then extensive work has

been carried out in Al-Fe-Cu system to understand the formation, phase stability, structure and the properties of this phase in order to exploit it for possible industrial applications, as the components of this system are relatively cheaper and easily available. The nature and concentration of minor elements in alloy affect significantly the properties of quasicrystals [12,13], for example, in Al–Cu–TM, (TM = transition metal), TM decides the type of quasicrystals. Co, Rh, Ni favour the formation of decagonal quasicrystals and Cr, Mn, Fe, Ru and Os favour the formation of icosahedral quasicrystals [14-17]. While Mn, Co, Fe, Ru, Os form stable quasicrystalline phase, with other TMs the phase is metastable. From the above, it is clear that the type of transition metals is the deciding factor in the quasicrystalline phase stability and therefore it is expected that substitution of Fe in place of Cr will make significant effect on the formation of various quasicrystalline phases. However, it is believed that in many intermetallics including quasicrystals, the combined effect of two elements shows the better properties. Liu et al [18] have shown that Al–Cu–Fe system exhibits the face-centred icosahedral while Al–Cu–Cr system corresponds to the primitive, icosahedral phase. After partial substitution of Cr in Al-Cu-Fe system, the formation of decagonal phase increases [19-20]. It is known that QC phase in Al-Cu-Fe undergoes a structural transformation to various types of crystalline phases during annealing, ion milling, electron beam irradiation and mechanical testing [21-24]. Mukhopadhyay et al [25-26] and Yadav et al [27] have studied the phase stability of pre-alloyed Al-Cu-Co and Al-Ni-Fe decagonal quasicrystalline (DQC) and Al-Cu-Fe icosahedral quasicrystalline material during MM. Therefore, the effect of MM in Al-Cu-Fe-Cr decagonal quasicrystal in regards to the phase stability is an interesting issue.

The aim of the present study was to synthesize a nanophase microstructure by mechanical milling (MM) of the DQC phase in the Al-Cu-Fe-Cr system and to study the phase stability.

Experimental Procedure

Synthesis

The alloy with a composition close to $Al_{65}Cu_{20}Fe_8Cr_7$ (Al=99.98%, Cu=99.99%, Fe = 99.98 %, Cr=99.97% pure) was was prepared by melting in a radio frequency induction furnace under a dry argon atmosphere. The individual elements were at first mixed in correct stoichiometric proportions and pressed into a cylindrical pellet of 2 cm diameter and 0.75 cm thickness by applying a pressure of ~ 3×10^4 N/m². The pellet (5 g by weight) was then placed in a silica tube surrounded by an outer Pyrex

ξ email: yadavtp@gmail.com

glass jacket. Under continuous flow of argon gas into the silica tube, the pellet was melted using R.F. induction furnace (18 kW). The ingots formed were re-melted several times to ensure homogeneity. This pre-alloyed as-cast ingot was crushed to particles less than 0.5 mm in size and placed in an attritor ball mill (Szegvari Attritor) with ball to powder ratio of 40:1. The attritor has a cylindrical stainless steel tank of inner diameter 13 cm. The grinding balls made of stainless steel are of 6 mm diameter. The speed of the mill was maintained at 400 rpm. The milling operation was conducted for various time ranging from 5 to 100 h using hexane as a process control agent (PCA)

Structural Characterization

The mechanically milled and annealed sample were subjected to structural characterization employing powder X-ray diffraction (XRD) Philips PW 1710 diffractometer with CuK_α radiation, λ = 1.5418 Å. The experimental conditions such as rating of X-ray generator (30 kV, 20 mA) and other diffractometer parameters such as scanning speed, were kept constant for all diffraction experiments performed on different samples, Differential thermal analysis (DTA) was carried out with heating rate of 10 °C/min. Sample thus prepared were studied by TEM using a Tecnai 20 G^2 at 200kV electron microscope employing imaging and diffraction modes.

The grain size and the lattice strain of the sample was calculated from the integral width of the physical broadening profile. Cauchy and Gaussian components were obtained from the ratio of full width at half maximum intensity (2ω) and integral breadth (β) [28]. In a single line analysis the apparent crystallite size 'D' and strain 'e' are related to Cauchy (β_c) and Gaussian (β_G) widths of the diffraction peak at the Bragg angle θ;

$$D = k\lambda / \beta_c \cos\theta \tag{i}$$

and

$$e = \beta_G / 4 \tan\theta \tag{ii}$$

The constituent Cauchy and Gaussian components are given as

$$\beta_c = (a_0 + a_1\psi + a_2\psi2)\beta$$

$$\beta_G = (b_0 + b_{1/2}(\psi - 2/\pi)_{1/2} + b_1\psi + b_2\psi2)\beta$$

where a_0, a_1 and a_2 are Cauchy constants, b_0, $b_{1/2}$, b_1 and b_2 are Gaussian constants and $\psi = 2\omega/\beta$ where β is the integral breadth obtained from XRD peak. The values of Cauchy and Gaussian constant have been taken from the table of Keijser *et al* [29] : a_0 = 2.0207, a_1 = 0.4803, a_2 = 1.7756; b_0 = 0.6420, $b_{1/2}$ = 1.4187, b_1 = 2.2043, b_2 = 1.8706 From these, we have calculated the crystallite size D and the lattice strain 'e' for the milled $Al_{65}Cu_{20}Fe_8Cr_7$ alloy.

Results and Discussion

Rigorous transmission electron microscopic investigation by obtaining selected area diffraction patterns and microstructural features at different stages have been carried out. Figure 1(a) show the microstructure of the decagonal quasicrystal and corresponding diffraction patterns can be seen in Fig. 1(b)-(c). The microstructure is a single-phase decagonal quasicrystal

having two different rotational axes as indicated in the Fig 1(a). The diffraction patterns of the decagonal phase characterized by its 10-fold, two fold patterns are shown in Fig 1(b) and 1(c). The two fold diffraction pattern of decagonal phase shows the presence of streaking along the aperiodic direction as shown in Fig. 1(c).These streaks can be interpreted due to disordering along decagonal axis.
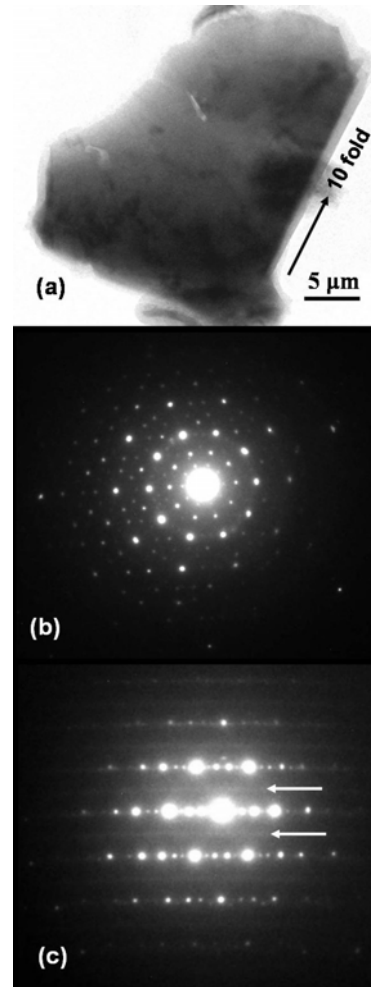

Figure 1. (a) TEM micrograph of as-cast alloy showing the decagonal phase of the order of μm in size, Ten fold and two fold (b-c)diffraction pattern confirms the formation of DQC

Figure 2 shows the XRD patterns obtained from the as-cast and milled powder samples. Figure 2(a) shows XRD pattern of the decagonal phase obtained from the as-cast $Al_{65}Cu_{20} Fe_8Cr_7$ alloy. The diffraction pattern corresponding to decagonal phase can be indexed by using six independent indices as proposed by Mukhopadhyay and Lord [30]. All of the peaks are from the decagonal phase, no other phase was identified. Figure 2(b) shows the XRD pattern from 40 h MM powder exhibiting broadening of the peaks belonging to the B2 phase. The B2 phase is a CsCl structure in intermetallics, its unit cell contains two different atoms located respectively on the vertex and the centre of a cube. Its lattice parameter is 0.29 ~0.31 nm.

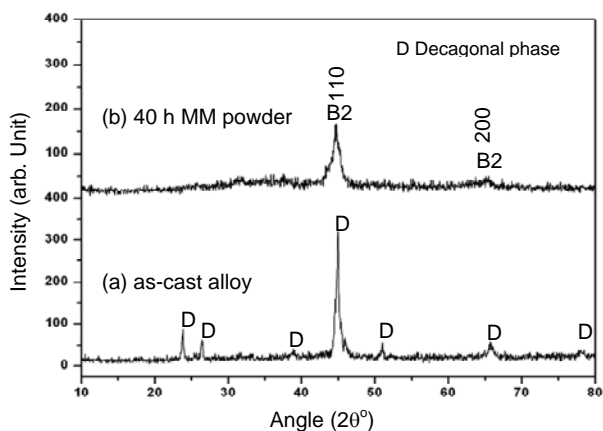Figure 2. X-ray diffraction pattern obtained from the as-cast $Al_{65}Cu_{20}Fe_8Cr_7$ alloy showing the formation of decagonal phase (curve 'a') and 40 h mechanical milled powder (curve 'b'), peak broadening corresponding to 110 curve indicates the formation of nano-B2 phase
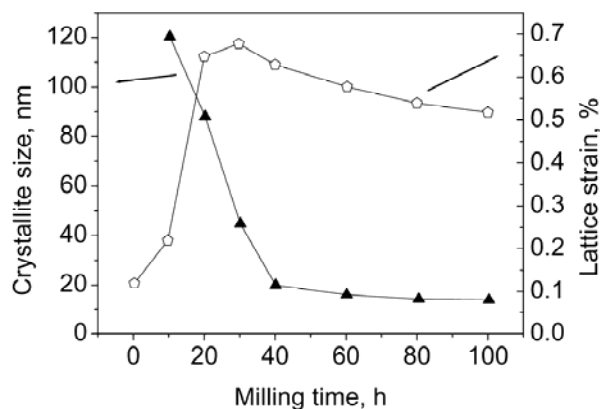

Figure 3. The variation of crystallite size and lattice strain with milling time
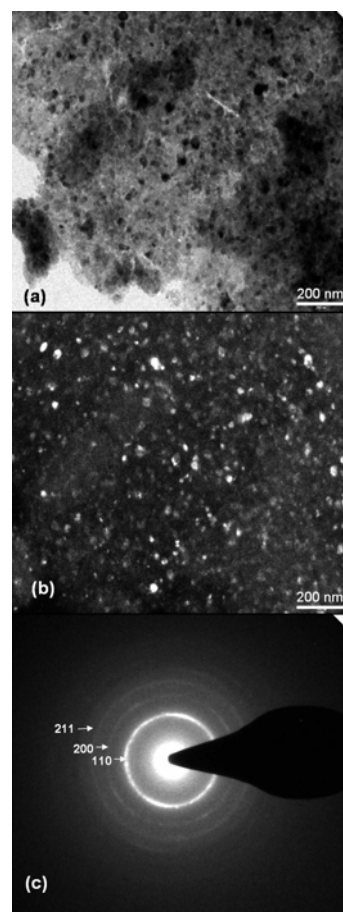

Figure 4. (a) Bright field and (b) dark field TEM images of powder sample after 40 h milling showing the aggregates of nano decagonal phase of the order of 12-20 nm in size, (c) the corresponding diffraction pattern of the nano B2 phase.

It can be seen that, with the milling proceeding, the reflection peak intensities of the milled samples are decreased and the peaks are significantly broadened, suggesting that a large amount of defects were introduced into the samples by mechanical attrition and finally the reduction of crystallite size. Often, sufficient information about the changes in grain size and lattice strain can be gained from the integrated width of the peaks, which must assume a model for the functional dependence of the grain size, lattice strain and instrumental broadening on the diffraction angle. The instrumental broadening profiles, determined by means of the Si reference sample in the present work, are revealed to be Gaussian function. We can get the physical profile of the 40 h milled powder, which is the convolution of size broadening with the strain broadening profile, by removing the instrumental broadening effect from the measured intensity profile. Both theory and experiment support the approximation of size broadening profiles by a Lorentzian function and strain broadening by a Gaussian function [27]. The crystallite size and the lattice strain of the sample were calculated from the integral width of the physical broadening profile. The detailed method of calculation is given in the experimental section. Figure 3 shows the overall variation of crystallite size and lattice strain with milling time. The lattice strain initially increases from 0.1 to 0.68 % at a rapid rate (at 30h milling) and then decreases further from 0.68 to 0.52 % at a slower rate. The distinct transition can be noticed. The variation of crystallite size with milling time is also shown in Fig. 3. From this plot it is clear that the crystallite size decreases from 120 nm to 18 nm at a faster rate and then down to 12 nm at a relatively slower rate during milling operation.

Figures 4 (a) and (b) are bright-field and dark-field TEM images obtained from the powder sample milled for 40 h. Some of the powder particles were electron transparent near the edges. The very fine grain size of the B2 phase, of the order of 10-20 nm, is evident. Figure 4(c) shows a typical ring diffraction pattern obtained from the sample. These rings can be indexed as the disordered B2 that is a bcc phase with a lattice parameter of 0.29 nm. However, no superlattice spot was found in the SADP. This is consistent with the observations from the XRD patterns.

The powder after the milling was analyzed by an energy-dispersive X-ray (EDX) Link system Tecnai 20 G^2 operating at 200 kV. The composition was found to be close to the nominal composition corresponding to the $Al_{65}Cu_{20}Fe_8Cr_7$ (Fig. 5). Some compositions variation was observed at different places. However,

the average composition appears to be not more than 0.5 at% in this powder. The composition from the statistical averages of several readings was found to be within ~ 2 % of the as-cast ingot composition. The total amount of transition metals, that is Fe, Cu, Ni and Cr, in powder milled for 40 h was estimated to increase by approximately 0.75 at.%, owing to pick-up of Fe and Cr from the stainless steel balls during milling.
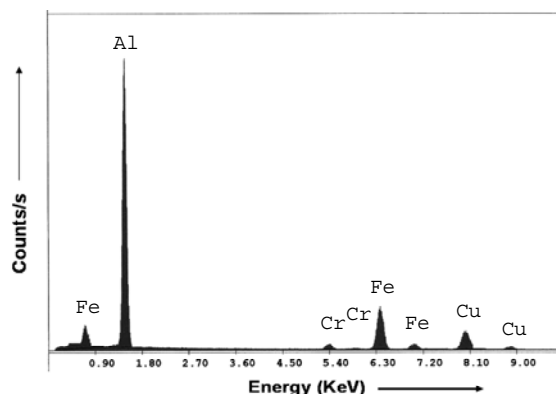

Figure 5. Energy-dispersive spectrum (EDX) from the 40 h MM $Al_{65}Cu_{20}Fe_8Cr_7$ powder

A more detailed study of the kinetics of the transformation, including the degree of ordering and grain coarsening, is under investigation. In addition, isothermal treatments at higher temperatures are being carried out to estimate the stability region of the B2 and DQC phases. Essentially, the role of MM is to lead to the enhancement of thermally activated diffusion by generating a large number of defects as well as forcing the atoms or groups of atoms to move from place to place. As it is possible to obtain a nanoscale microstructure, the rate of diffusion during subsequent thermal heat treatment is quite high, which may lead to the formation of equilibrium or stable phases in the system. In the present investigation it was found that the QC phase was unstable during milling, transforming to nanocrystals of the B2 phase.

Conclusions

From the present study, we can conclude that the DQC phase in $Al_{65}Cu_{20}Fe_8Cr_7$ is unstable under high-energy ball milling, transforming to a nanocrystalline B2 phase. The repeated impact between the balls and powders appears to cause the generation of various types of defects including phason type. Consequently, due to the defects generated during milling, the structural transformation to a crystalline phase takes place. On milling up to 40 h, grain refinement via two stages is achieved and the grain size reached to a minimum of 14 nm. The lattice strain accumulation is found to increase initially at a high rate and then at slower rate. The grain refinement and strain accumulation via two stages have been explained by a change of deformation mechanism operating during milling.

Acknowledgement

References

1. B.S. Murty and S. Ranganathan, *International Materials Reviews,* 43 (1998) 101.
2. A. Calka and D. Wexlex, *Nature,* 419 (2002) 147.
3. C.C. Koch, *Annu. Rev. Mater Sci.*, 18 (1989) 121.
4. C. Surganarayana, *Progress in Materials Science,* 46 (2001)1.
5. T.P. Yadav, N.K. Mukhopahdyay, R.S. Tiwari and O.N. Srivastava, *Trans IIM,* 58 (2005) 1169.
6. C.C. Koch and J.D. Whittenberge, *Intermetallics,* 4 (1996) 339.
7. F. Tang, H. Meeks, J.E. Spowart, T. Gnaeupet - Herold, H. Prask and I.E. Anderson, *Materials Science and Engineering A,* 386 (2004) 194.
8. D. Shechtman, I Blech, D. Gratias, and J.W Cahn, *Phys.Rev. Lett,.* 53 (1984) 951.
9. K. Chattopadhyay, S. Lele and S. Ranganathan, *Acta. Met.,* 35 (1987) 727.
10. E.H. Saarivirta, *J. Alloys and Compounds,* 363 (2004) 150.
11. A.P. Tsai, A. Inoue, and T. Masumoto, *Mater. Trans. Japan Inst. Metals,* 30 (1989) 300.
12. A. Singh and S. Ranganathan, *Metals, Mater. & Process.,* 2 (1991) 4.
13. V. Khare, R.S. Tiwari and O.N. Srivastava, *Bull. Mater. Sci., 24* (2001)257.
14. A.P. Tsai, A. Inoue and T. Masumoto, *J. Mater. Sci. Lett.,* 7 (1988) 322.
15. A.P. Tsai, A. Inoue and T. Masumoto *Mater. Trans.,* 30 (1989) 300.
16. L.X. He, Y.K. Wu and K.H. Kuo, *J. Mater. Sci. Lett.,* 7 (1988) 1284.
17. L.X. He, Y.K. Wu, X.M. Meng and K.H. Kuo, *Phil. Mag. Lett.,* 61 (1990) 51.
18. W. Liu, U. Köster, F. Müller and M. Rosenberg, *Phys. Status Solidi, (a)* 132 (1992) 17.
19. G. Bonhomme M. LeMieux P. Weisbecker V.V. Tsukruk and J.M. Dubois *Journal of Non-Crystalline Solids*, 334 & 335 (2004) 532.
20. G. Rosas and R. Perez, *Journal of Materials Science,* 32 (1997) 2403.
21. S. Ebalard, and F. Spaepen, *J. Mater. Res.,* 5 (1990) 62.
22. H. Zhang, K. Urban, *Phil. Mag. Lett.,* 66 (1992) 209.
23. S.S. Kang, and J.M. Dubois, *Europhys. Lett.,* 18 (1992) 45.
24. J.S. Wu, V. Brien, P. Brunet, C. Dong, and J.M. Dubois, *Phil. Mag. A,* 80 (200) 1645.
25. N.K. Mukhopadhyay, G.V.S. Murthy, B.S. Murty, and G.C.Weatherly, *Phil. Mag. Lett.,* 82 (2002) 383.
26. N.K. Mukhopadhyay, T.P. Yadav, and O.N. Srivastava, *Phil. Mag. A,* 82 (2002) 2979.
27. T.P. Yadav N.K. Mukhopadhyay, R.S. Tiwari and O.N. Srivastava, *Phil. Mag.*, 86 (2006) 397.
28. T.P. Yadav N.K. Mukhopadhyay, R.S. Tiwari and O.N. Srivastava, *Materials Science and Engineering A, 393* (2005) 366.
29. Th.H.de Keijser, J.I. Langford, E. J. Mittemeijer and A. B. P. Vogels, *J. Appl. Cryst.,* 15 (1982) 308.
30. N.K Mukhopadhyay and E.A Lord, *Acta. Cryst. A,* 58 (2002) 424.